Supplemental Information

Kti12, a PSTK-like tRNA dependent ATPase essential for tRNA modification by Elongator

Rościsław Krutyhołowa[1,2§], Alexander Hammermeister[3§], Rene Zabel[4#], Wael Abdel-Fattah[3$], Annekathrin Reinhardt-Tews[4], Mark Helm[5], Michael J. R. Stark[6], Karin D. Breunig[4], Raffael Schaffrath[3*] and Sebastian Glatt[1*]

[1] Max Planck Research Group at the Malopolska Centre of Biotechnology, Jagiellonian University, Krakow, Poland

[2] Department of Cell Biochemistry, Faculty of Biochemistry, Biophysics and Biotechnology, Jagiellonian University, Krakow, Poland

[3] Institut für Biologie, FG Mikrobiologie, Universität Kassel, Kassel, Germany

[4] Institute of Biology, Martin Luther University Halle-Wittenberg, Halle (Saale), Germany

[5] Institut für Pharmazie und Biochemie, Universität Mainz, Mainz, Germany

[6] Centre for Gene Regulation & Expression, University of Dundee, Dundee, UK

§ these authors contributed equally

[$] present address: Department of Medical Biochemistry and Biophysics, Umeå University, Sweden

[#]present address: serYmun Yeast GmbH, Halle (Saale), Germany

* Correspondence to RS (schaffrath@uni-kassel.de) and SG (sebastian.glatt@uj.edu.pl)

Keywords: Kti12, tRNA modifications, Elongator, PSTK, selenocysteine, ATPase

Running title: Kti12, a PSTK-like regulator of Elongator

Supplemental Figures

Supplementary Figure S1
Kti12 purification and structure determination.

Supplementary Figure S2
tRNA binding mode of Kti12.

Supplementary Figure S3
Analysis of ATPase activity of Kti12.

Supplementary Figure S4
Influence of nucleoside triphosphates on Kti12.

Supplementary Figure S5
Properties of the tRNA interacting surface of Kti12.

Supplementary Figure S6
***In vivo* and *in vitro* studies of Kti12 function in the Elongator pathway for U_{34} modification.**

Supplemental Tables

Supplementary Table S1 (suggested as Appendix Table 1)
List of used strains.

Supplementary Table S2 (suggested as Appendix Table 2)
Mass-spectrometry.

Supplementary References (SI only)

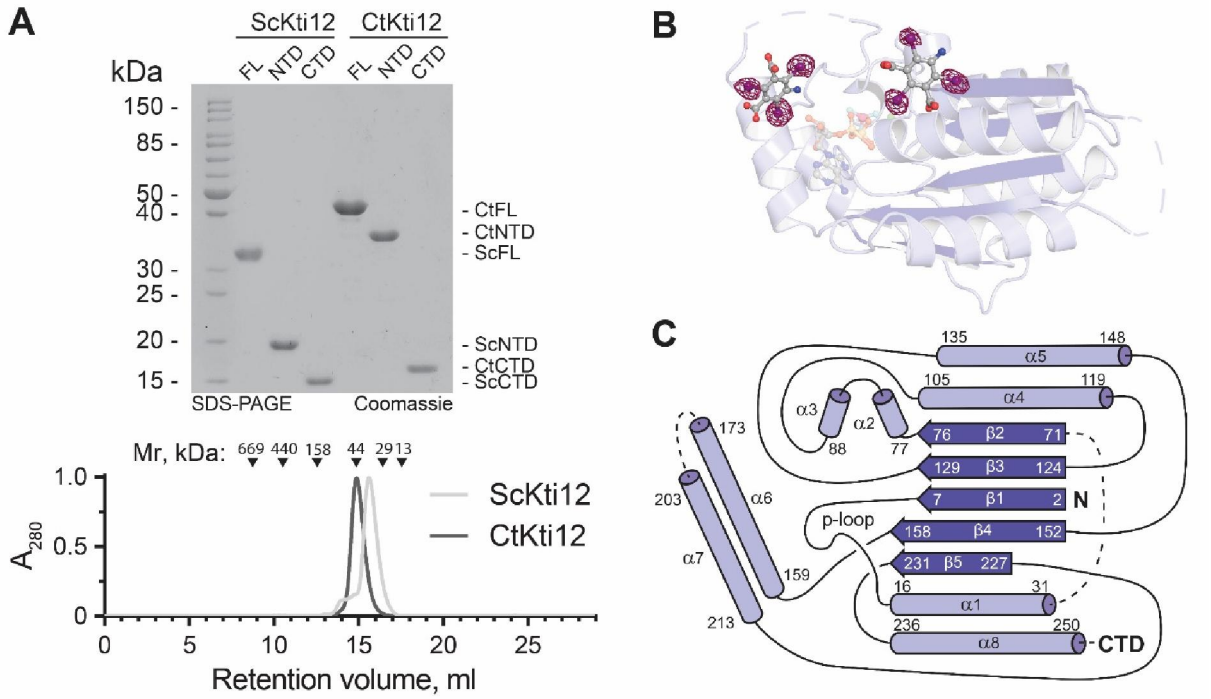

Supplementary Figure S1. Kti12 purification and structure determination.

A. Purity of the studied proteins (full-length [FL], N-terminal [NTD] and C-terminal domains [CTD] of both ScKti12 and CtKti12) assessed using 12% SDS-PAGE (top panel) and gel filtration profiles (bottom panel) of ScKti12$_{FL}$ and CtKti12$_{FL}$ separated on an S200 column. CtKti12 exhibits purely monomeric behavior. The additional shoulder observed in case of ScKti12 is likely caused by the low solubility of the purified ScKti12$_{FL}$ protein.

B. Anomalous difference Fourier map plotted on Kti12$_{NTD}$ structure. Isomesh represents an electron density map at σ = 5.0 visualized in a vicinity of CtKti12$_{NTD}$. Two magic triangle molecules, each containing 3 iodine atoms (violet spheres), precisely fit into identified densities.

C. A topological map of CtKti12$_{NTD}$. Helices are shown as light blue cylinders; β-strands are shown as darker arrows. A P-loop motif significant for ATP hydrolysis is shown.

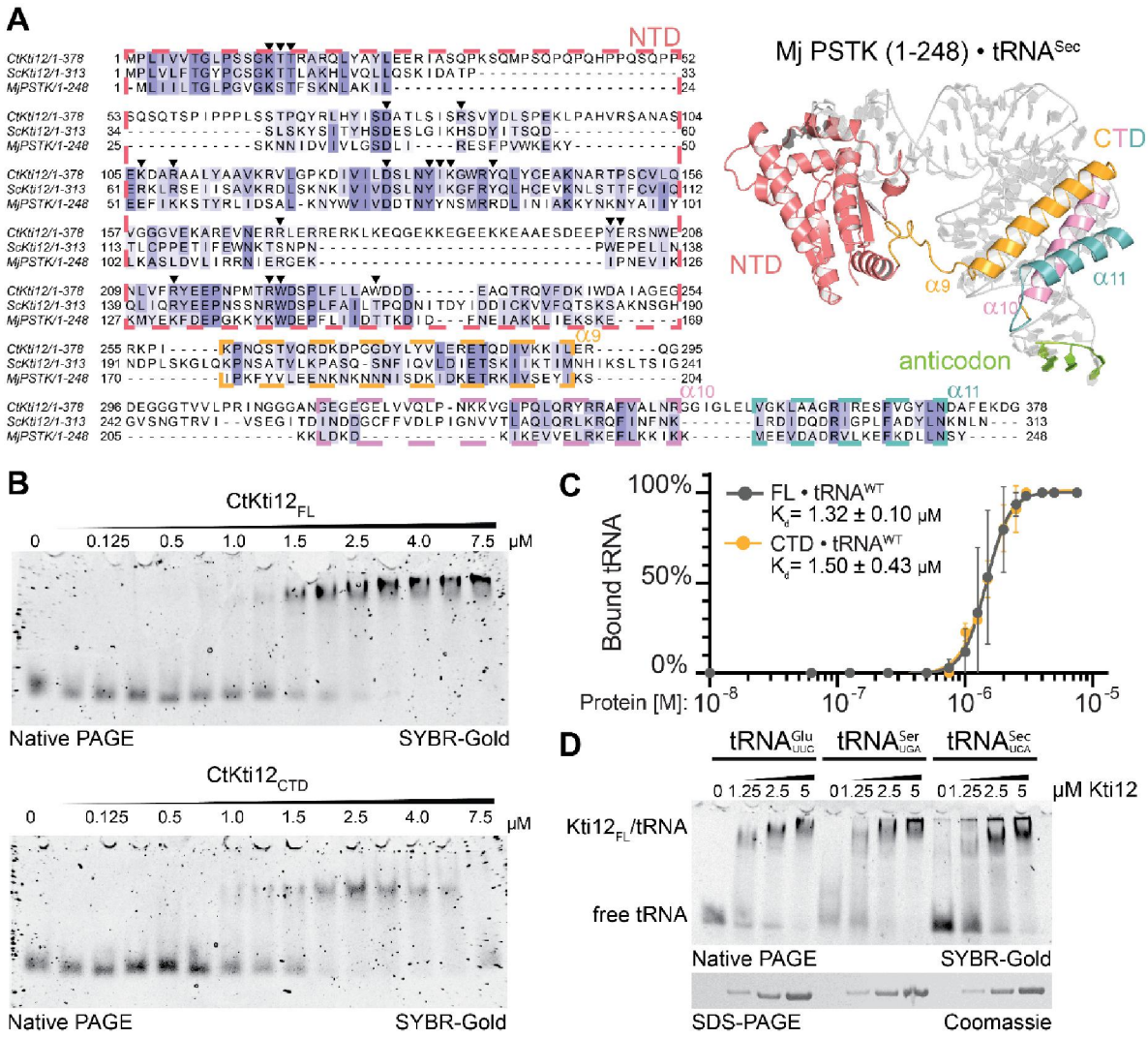

Supplementary Figure S2. tRNA binding mode of Kti12.

A. Structure-based sequence alignment of CtKti12, ScKti12 and MjPSTK. All three proteins share a high degree of sequence identity and architectural resemblance. The ATPase domain is shown in red, helices α9, α10 and α11 are shown in yellow, violet and cyan respectively. Residues mutated in CtKti12 for the purpose of the current study are highlighted with black triangles. Alignment was prepared using Jalview software (1). (Top right): To highlight structural features of these motifs the same color code was applied to the structure of MjPSTK (PDB ID 3ADB, single PSTK protein is shown, tRNA is colored in grey, anticodon is highlighted with green).

B. Representative electrophoretic mobility shift assays (EMSA) used for experimental K_D determination of $CtKti12_{FL}$ and $CtKti12_{CTD}$. Protein concentration ranged from 0.06 μM to 7.5 μM. Yeast bulk $tRNA^{WT}$ (0.11 μM) was used as substrate.

C. Quantification of free tRNA and tRNA in complex with $CtKti12_{FL}$ or $CtKti12_{CTD}$ respectively, formed during the course of experiments shown in (B) and showing fitted binding curves. The dissociation constants (K_d) were calculated from three replicated experiments (n=3).

D. Binding affinity of $CtKti12_{FL}$ to *in vitro* transcribed tRNA ($SctRNA^{Glu}_{UUC}$, $SctRNA^{Ser}_{UGA}$ and $HstRNA^{Sec}_{UCA}$). Increased concentration of protein was incubated with 0.22 μM of the indicated tRNA and subjected to EMSA on a 5% native PAGE. As a loading control, samples were also analyzed by denaturing SDS-PAGE. tRNA was stained using SYBR-Gold.

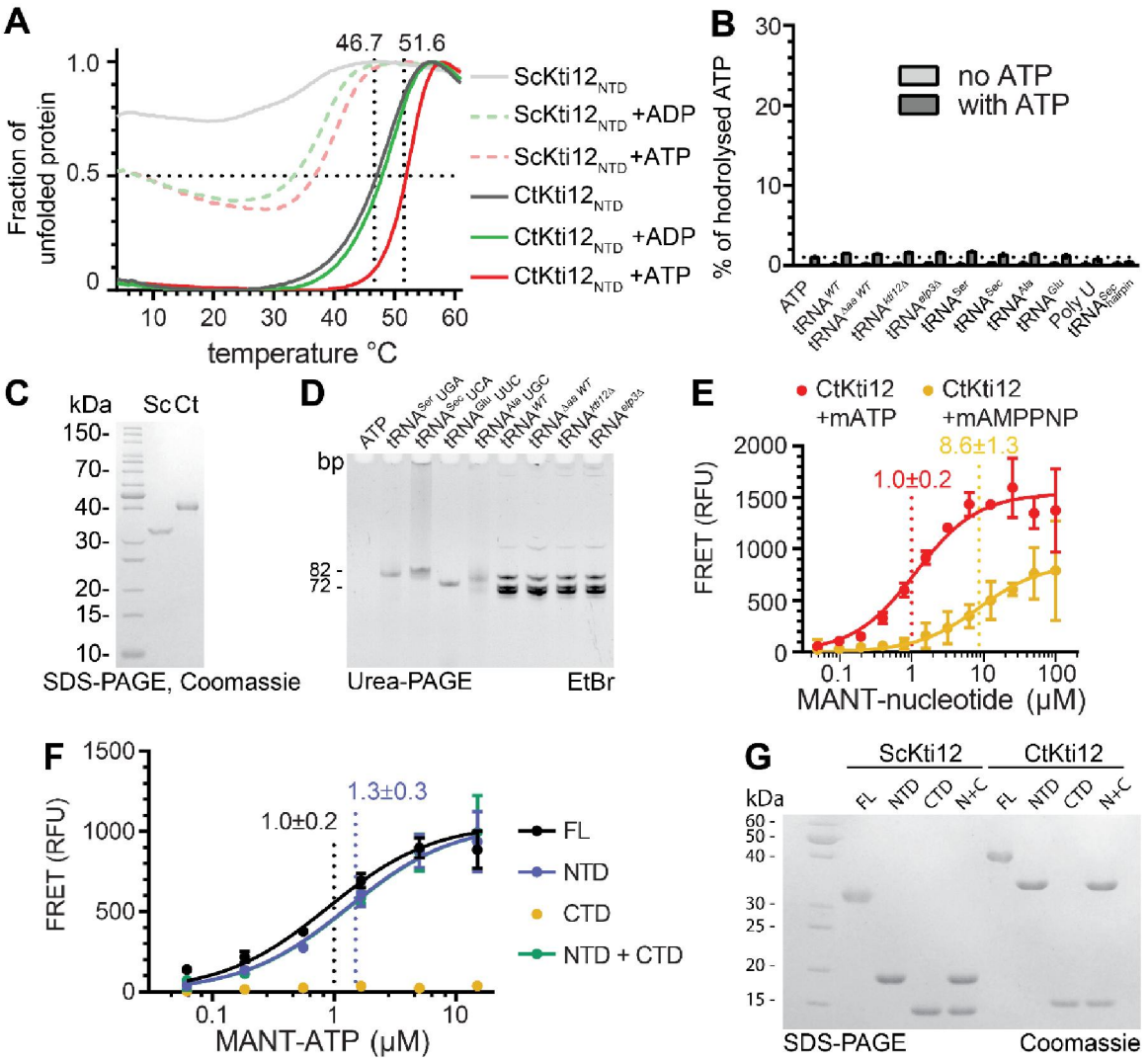

Supplementary Figure S3. Analysis of ATPase activity of Kti12.

A. Thermal shift assays for ScKti12$_{NTD}$ and CtKti12$_{NTD}$. The denaturation temperatures determined are similar to the ones measured for FL proteins. Both NTDs exhibit ATP-dependent thermostabilization. In case of ScKti12$_{NTD}$, the initial unfolded fraction is high illustrating limited solubility of the construct.

B. Malachite green assay showing that tRNA species used in Figure 2C were free of any contaminations capable of hydrolyzing ATP. Bars correspond to the mean of three independent experiments ± standard deviation.

C. Protein input control for the malachite green assays shown in Figure 2C analyzed using 12% SDS-PAGE stained with Coomassie.

D. tRNA (used in Figure 2C) input and quality control. 5% Urea-PAGE stained with EtBr.

E. Analyses of nucleotide binding affinity of CtKti12. CtKti12 protein was incubated in a presence of mATP (MANT-ATP, red) or mAMPPNP (MANT-AMPNPN, yellow). FRET was induced using λ_{ex}: 280 nm; λ_{em}: 448 nm. RFU values after baseline subtraction are shown, error bars indicate standard deviations, (n=3).

F. Study of potential influence of CTD on nucleotide binding performed using MANT-ATP binding assay. NTD exhibits ATP binding affinity not significantly different from a FL CtKti12 protein. Addition of CTD to the NTD does not alter its affinity to ATP. FRET was induced as in (B). Mean RFU values after baseline subtraction are shown, error bars amount to standard deviation, (n=3).

G. Protein input control for the malachite green assay shown in Figure 2D.

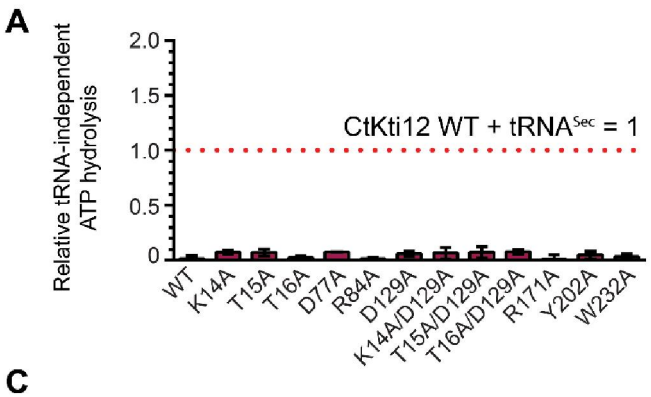

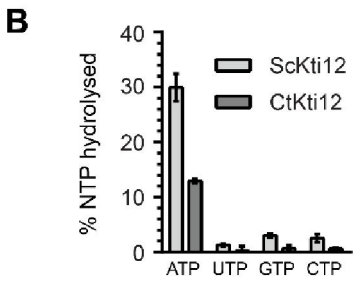

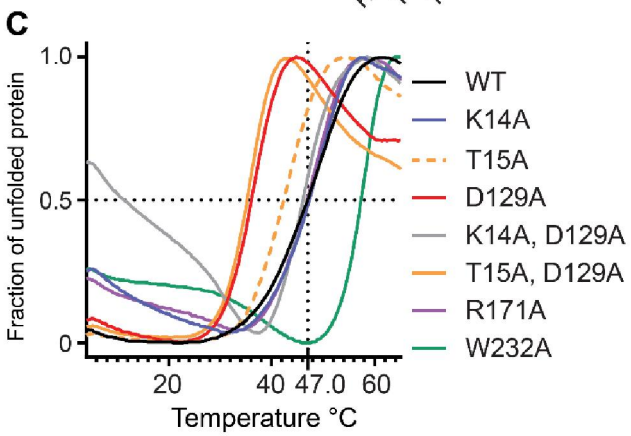

D

	Mean T_m, °C	ATP °C	ATP Kd, µM	ScKti12 Residue
WT	46.97 ± 0.64	4,8	1.0±0.2	
K14A	47.33 ± 0.95	-1	>15	K14
T15A	42.37 ± 1.18	0	>15	T15
T16A	47.93 ± 0.94	-0,8	2.2±0.3	T16
D77	47.45 ± 1.44	0	>15	D45
R84A	46.53 ± 1.35	0	>15	H52
D129A	36.03 ± 0.54	0	>15	D85
K14A/D129A	46.00 ± 0.95	0	>15	K14/D85
T15A/D129A	35.17 ± 0.39	0	>15	T15/D85
T16A/D129A	37.23 ± 0.23	-1,3	>15	T16/D85
R171A	46.83 ± 0.61	-1,4	4.7±1.1	K125
Y202A	43.30 ± 0.87	0,5	7.0±2.1	W132
W232A	57.30 ± 0.43	0	5.4±1.6	W123

Supplementary Figure S4. Influence of nucleoside triphosphates on Kti12.

A. Nucleotide binding pocket mutants exhibit almost no tRNA-independent ATP hydrolysis in the absence of $tRNA^{Sec}$.

B. Ability of Kti12 proteins to hydrolyze other nucleoside triphosphates was analyzed using malachite green assay. Unlike MjPSTK, both ScKti12 and CtKti12 exhibited a significant preference for ATP. Bars correspond to the mean of three independent experiments ± standard deviation.

C. Stability of nucleotide binding pocket mutants examined by thermal shift assays. K14A and R171A exhibit similar stability to the WT protein. Thermostability of the T15A mutant is slightly affected. Mutation of D129 to alanine in the WT and T15A substitution resulted in potent protein destabilization, decreasing thermal stability by 10 °C. Thermostability of K14A/D129A double mutant is close to the WT protein. Thermostability of W232A was significantly improved.

D. Detailed numerical thermal shift data for all nucleotide binding pocket mutants with corresponding residues in ScKti12. Red highlights destabilized mutants whereas green indicates stabilization. Column “ATP °C” represents thermal shifts of nucleotide binding pocket mutants upon stimulation with ATP in the absence of tRNA, red corresponds to lack of ATP-dependent thermostabilization. Column “ATP Kd, µM” provides Kd values for mutants obtained from MANT analysis. In multiple cases measurement was not possible within proposed concentration range, thus, Kd is located beyond measured gradient, what is indicated by “> 15” label. Red indicates more than two-fold difference in ATP binding in comparison to the WT protein.

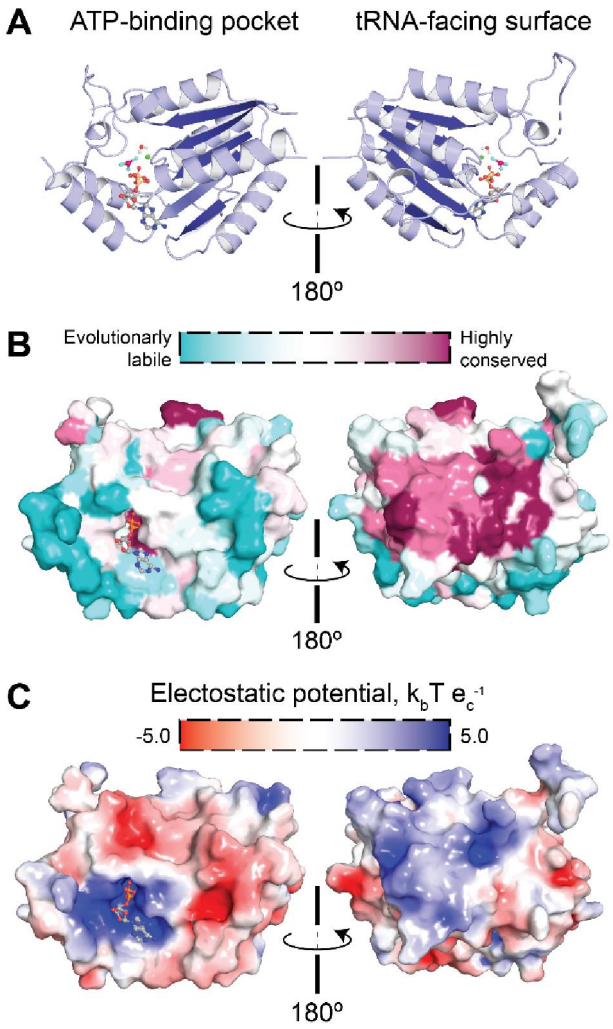

D

	Mean Tm, ˚C	ATP °C	ATP Kd, μM	Residue in ScKti12
WT	46.97 ± 0.64	4,8	1.0±0.2	
K106A/R109A	48.97 ± 0.69	0	5.4±1.0	R62/R65
Y133A/I134A	46.97 ± 0.66	1	2.9±0.6	Y89/I90
K135A	46.67 ± 0.43	5,6	1.0±0.2	K91
Y139A	43.67 ± 0.87	4,9	1.9±0.5	Y95
E203A	46.87 ± 0.88	1,8	1.0±0.2	E133
R213A	44.27 ± 0.67	1,3	1.9±0.3	R143
R222A/W223A	47.00 ± 0.18	4	0.9±0.2	R152/W153

Supplementary Figure S5. Properties of the tRNA interacting surface of Kti12.

A. Front and back view of $CtKti12_{NTD}$ shown in a ribbon representation.

B. Conservation of $CtKti12_{NTD}$ surface assessed in relation to 17 Kti12 proteins from distant model species, namely: *Chaetomium thermophilum, Saccharomyces cerevisiae, Candida albicans, Arabidopsis thaliana, Nicotiana tomentosiformis, Oryza sativa Japonica Group, Physcomitrella patens, Danio rerio, Xenopus laevis, Drosophila melanogaster, Mus musculus, Rattus norvegicus, Felis catus, Bos taurus, Pan troglodytes, Macaca mulatta* and *Homo sapiens*. Conservation visualization was performed using ConSurf server (2). Both the nucleotide binding pocket and the tRNA interaction surface display a high degree of evolutionary conservation indicating the importance of the relevant amino acid residues for proper functioning of the Kti12 protein.

C. Electrostatic potential of CtKti12$_{NTD}$ calculated using APBS module of PyMol at 300 K (3). The molecule was prepared using pdb2pqr method. The surface represents solvent excluded surface (Conolly surface). Electrostatic surface charge ranges from -5.0 units (red, negative charge) to 5.0 units (blue, positive charge). The tRNA interacting region of Kti12 exhibits a significant positive charge that can be exploited for electrostatic attraction of a negatively charged tRNA phosphate backbone.

D. Thermal shift assay data for tRNA-interaction surface mutants. Column “ATP °C” provides thermal shift data for tRNA-interaction surface mutants upon stimulation with ATP in the absence of tRNA, red corresponds to the lack of ATP-dependent thermostabilization. Column “ATP Kd, μM” provides Kd values for mutants obtained by the means of MANT analysis. Red indicates more than two-fold difference in ATP binding in comparison to the WT protein.

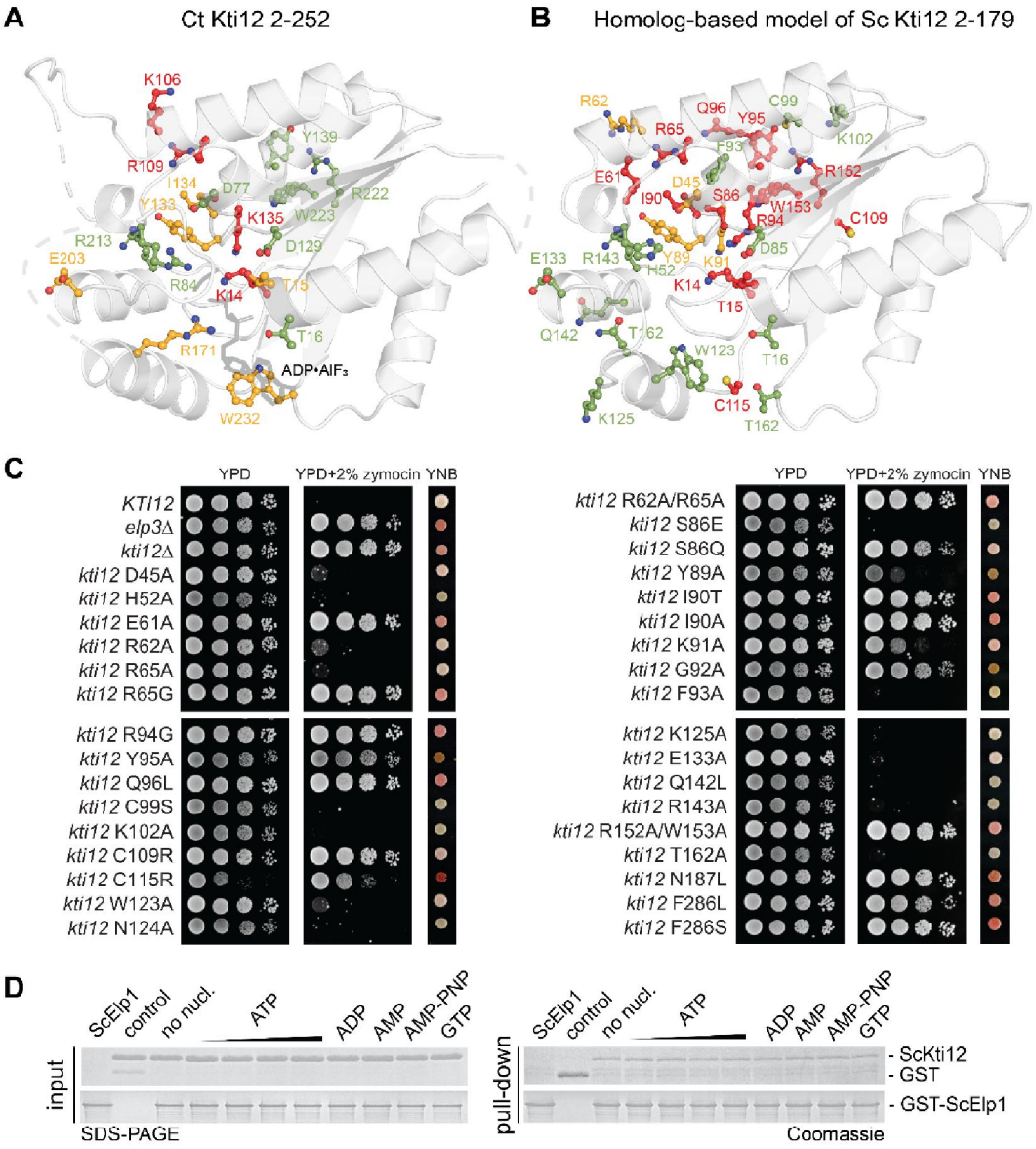

Supplementary Figure S6. *In vivo* and *in vitro* studies of Kti12 function in the Elongator pathway for U_{34} modification.

A. A structural overview of mutations within NTD of CtKti12. Residues highlighted with red are crucial for tRNA-induced ATP hydrolysis, orange residues result in a moderate decrease of ATP hydrolysis. Mutations of green residues have weak or no effect on ATP hydrolysis by CtKti12.

B. A homolog-based model of $ScKti12_{NTD}$ based on a structure of $CtKti12_{NTD}$ generated using the SWISS-MODEL server (4). Mutations leading to a robust zymocin resistance phenotype are shown in red, those leading to a moderate phenotype are shown in orange and mutations conferring a WT phenotype are shown in green.

C. Phenotypes of yeast strains carrying the indicated mutations using the zymocin sensitivity *SUP4* (*ade2-1*) assays (described in the Methods).

D. Kti12 interacts with the Elongator subunit Elp1 in a nucleotide-independent manner. Interaction between the purified proteins was studied using a GST pull-down assay and visualized by 12% SDS-PAGE. The concentration of all nucleotides or their non-hydrolysable analogs was kept at 1 mM. The ATP gradient covered 1 μM, 10 μM, 100 μM and 1 mM concentrations. The buffer contained 20 mM Tris-HCl pH 7.5, 150 mM NaCl, 2 mM DTT and 2 mM $MgCl_2$ and 0,5% v/v Tween 20.

Supplementary Tables

Supplementary Table S1. Used yeast strains.

Strain	Relevant genotype	Source
UMY2893	*MATα SUP4 leu2-3,112 trp1-1 can1-100 ura3-1 ade2-1 his3-11,15*	Huang et al. 2005
UMY2916	UMY2893*, elp3Δ::KanMX4*	Huang et al. 2005
YAH76	UMY2893*, ELP1-(c-myc)$_3$::SpHIS5 kti12Δ::KlURA3*	This study
YAH3	UMY2893, *ELP1-(c-myc)$_3$::SpHIS5 KTI12-(HA)$_6$::KlTRP1*	This study
RZY144	YAH76, *kti12_K14A-(HA)$_6$::KlTRP1*	This study
RZY145	YAH76, *kti12_T15A-(HA)$_6$::KlTRP1*	This study
YAH95	YAH76, *kti12_T16A-(HA)$_6$::KlTRP1*	This study
YAH80	YAH76, *kti12_D45A-(HA)$_6$::KlTRP1*	This study
YAH82	YAH76, *kti12_H52A-(HA)$_6$::KlTRP1*	This study
YAH94	YAH76, *kti12_E61A-(HA)$_6$::KlTRP1*	This study
YAH82	YAH76, *kti12_R62A-(HA)$_6$::KlTRP1*	This study
YAH83	YAH76, *kti12_R65A-(HA)$_6$::KlTRP1*	This study
RZY107	YAH76, *kti12_R65G-(HA)$_6$::KlTRP1*	This study
YAH84	YAH76, *kti12_R62A/R65A-(HA)$_6$::KlTRP1*	This study
RZY150	YAH76, *kti12_D85A-(HA)$_6$::KlTRP1*	This study
RZY151	YAH76, *kti12_T15A/D85A-(HA)$_6$::KlTRP1*	This study
RZY147	UMY2893, *kti12_S86E-(HA)$_6$::KlTRP1*	This study
RZY149	UMY2893, *kti12_S86Q-(HA)$_6$::KlTRP1*	This study
RZY159	YAH76, *kti12_Y89A-(HA)$_6$::KlTRP1*	This study
LGY02	UMY2893, *kti12_I90T-(HA)$_6$::KlTRP1*	This study
YAH85	YAH76, *kti12_Y89A/I90A-(HA)$_6$::KlTRP1*	This study
YAH92	YAH76, *kti12_K91A-(HA)$_6$::KlTRP1*	This study
RZY156	YAH76, *kti12_G92A-(HA)$_6$::KlTRP1*	This study
RZY160	YAH76, *kti12_F93A-(HA)$_6$::KlTRP1*	This study
YAH86	YAH76, *kti12_R94G-(HA)$_6$::KlTRP1*	This study
YAH93	YAH76, *kti12_Y95A-(HA)$_6$::KlTRP1*	This study
RZY157	YAH76, *kti12_Q96L-(HA)$_6$::KlTRP1*	This study
RZY155	YAH76, *kti12_C99S-(HA)$_6$::KlTRP1*	This study
RZY161	YAH76, *kti12_K102A-(HA)$_6$::KlTRP1*	This study
RZY44	UMY2893, *kti12_C109R-(HA)$_6$::KlTRP1*	This study
SBY04	UMY2893, *kti12_C115R-(HA)$_6$::KlTRP1*	This study
YAH87	YAH76, *kti12_W123A-(HA)$_6$::KlTRP1*	This study
RZY148	UMY2893, *kti12_N124A-(HA)$_6$::KlTRP1*	This study
YAH88	YAH76, *kti12_K125A-(HA)$_6$::KlTRP1*	This study
YAH89	YAH76, *kti12_E133A-(HA)$_6$::KlTRP1*	This study
RZY154	YAH76, *kti12_Q142L-(HA)$_6$::KlTRP1*	This study
YAH90	YAH76, *kti12_R143A-(HA)$_6$::KlTRP1*	This study
YAH91	YAH76, *kti12_R152A/W155A-(HA)$_6$::KlTRP1*	This study
RZY135	UMY2893, *kti12_T162A-(HA)$_6$::KlTRP1*	This study

Supplementary Table S2. Mass-spectrometry.

Modified nucleoside	Precursor ion m/z	Product ion m/z	Fragmentor voltage [V]	Collision energy [eV]	Cell accelerator voltage [V]	Retention time [min]	Δrt [min]
mcm^{5}s^{2}U	333	201	66	5	2	16.3	2
mcm^{5}U	317	185	66	5	2	12.7	2
ncm^{5}U	302	170	66	5	2	6.0	2
s^{2}U	261	129	66	5	2	11.3	2

Supplementary References (SI only)

1. Waterhouse,A.M., Procter,J.B., Martin,D.M.A., Clamp,M. and Barton,G.J. (2009) Jalview Version 2--a multiple sequence alignment editor and analysis workbench. *Bioinformatics*, **25**, 1189–1191.
2. Celniker,G., Nimrod,G., Ashkenazy,H., Glaser,F., Martz,E., Mayrose,I., Pupko,T. and Ben-Tal,N. (2013) ConSurf: Using Evolutionary Data to Raise Testable Hypotheses about Protein Function. *Isr. J. Chem.*, **53**, 199–206.
3. Jurrus,E., Engel,D., Star,K., Monson,K., Brandi,J., Felberg,L.E., Brookes,D.H., Wilson,L., Chen,J.H., Liles,K., *et al.* (2018) Improvements to the APBS biomolecular solvation software suite. *Protein Sci.*, **27**, 112–128.
4. Waterhouse,A., Bertoni,M., Bienert,S., Studer,G., Tauriello,G., Gumienny,R., Heer,F.T., de Beer,T.A.P., Rempfer,C., Bordoli,L., *et al.* (2018) SWISS-MODEL: homology modelling of protein structures and complexes. *Nucleic Acids Res*, **46**, W296--W303.